# Effect of microalloying on tempering of Mo-W high thermal conductivity steel

J. Burja, A. Nagode, J. Medved, T. Balaško, K. Grabnar

The effect of microalloying elements, niobium, tantalum and titanium on tempering, namely secondary hardening peaks was studied. The austenitisation temperatures, along with grain growth was studied. A high thermal conductivity hot-work tool steel was studied, with the following modifications Nb+0,06 w/% Nb, Ta+0,03 w/% Ta, and Ti+0,006 w/% Ti) based on reference (sample 0). Thermodynamic calculations were used to investigate the influence of microalloying on the transformation temperatures and carbide formation. The austenitisation temperatures of 1030, 1060, 1080 and 1100 °C were chosen and the samples were tempered at 540, 580, 600, 620 and 640 °C. The microstructure, hardness and grain size were investigated. The microalloying elements had a positive effect on grain size during austenitisation and on the increase of hardness during tempering. The microstructure was also investigated with electron microscopy. Mo-W carbides were dominant and showed coarsening and morphological changes, mainly rounding, during high temperature tempering. The secondary hardening peaks were reached at temperatures between 600 and 620 °C.

**KEYWORDS:** HOT WORK TOOL STEEL, MICROALLOYING, MOLYBDENUM, TUNGSTEN, TEMPERING, HEAT TREATMENT

## INTRODUCTION

Hot-work tool steels are a superior grade of steel known for their outstanding mechanical properties at high temperatures, making them essential for various applications. They are commonly utilized in the production of dies for extrusion, forging, and die casting. These dies undergo rigorous cyclic mechanical and thermal stresses, as well as abrasion, and adhesion. Therefore, hot work tool steels need exhibit combination of strength, hardness, toughness, wear resistance, thermo-cyclic stability, and good thermal conductivity [1-6]. The damage to these steels is primarily caused by a combination of low cycle fatigue and thermal fatigue resulting from frequent temperature fluctuations during operation [7,8].

Controlled chemical composition and appropriate heat treatment are necessary to achieve the required mechanical properties of hot-work tool steel. The typical microstructure of these steels consists of tempered martensite and carbide precipitates [9-12]. The heat treatment process involves three stages: austenitizing, quenching, and tempering. In the austenitization process, undissolved carbides, nitrides, or carbonitrides inhibit the growth of austenite crystal grains, which is essential for achieving small crystal grains and adequate mechanical properties. Microalloying elements such as Nb, Ta, V, and Ti are added to suppress grain growth [5,12,18]. Carbide precipitates, however, play a crucial role in secondary

Jaka Burja
Institute of Metals and Technology, Slovenia

Aleš Nagode, Jožef Medved, Tilen Balaško
Department of Materials and Metallurgy, Faculty of Natural Sciences and Engineering, University of Ljubljana, Slovenia

Klemen Grabnar
Beni Tehing d.o.o., Slovenia

hardening during tempering, with different carbide types forming depending on the chemical composition and tempering temperatures. However, above the maximum temperature for secondary hardening, carbides coarsen leading to softening of the steel [7]. The coarsening of carbides can be delayed to slow down the deterioration of the martensitic microstructure, maintaining high hardness and fatigue strength at higher temperatures and times. Therefore, understanding the microstructure evolution during tempering and service is crucial for controlling the tool life [22].

Previous studies have examined the impact of microalloying elements (V, Nb, or Ti) on the quenching and tempering process of low-alloy steels, as well as the composition and distribution of microalloyed carbides during tempering [14,23-25]. However, they have not studied the effect of microalloying elements on the tempering process of higher alloy steels that exhibit a secondary hardening peak, particularly Mo-W tool steels with high thermal conductivity values of up to 60 W·mK-1 [6,26,27]. Therefore, this study aims to investigate the effect of microalloying elements (Nb, Ta, and Ti) on the tempering process of Mo-W hot-work steel. The research will examine the role of microalloying elements in microstructural evolution and the development of secondary hardening peaks during tempering.

## MATERIALS AND METHODS

The experimental batches of the reference steel (0 – Tab. 1) were remelted in a vacuum induction melting furnace under 300 mbar argon. A total of four ingot measuring 60 x 60 x 400 mm and weighing 8 kg produced. The first batch of reference steel (0) was remelted without modification to the chemical composition. The second batch was remelted with the addition of 0.06 wt.% Nb (Nb – Tab. 1), the third batch was remelted with the addition of 0.03 wt.% Ta (Ta – Table 1) and the fourth charge was remelted with addition of 0.006 wt.% of Ti (Ti – Tab. 1). After casting, the ingots were cooled to room temperature in air. The microalloying additives were selected according to preliminary thermodynamic calculations. The aim was to form secondary carbides of the MC type in the austenite, but not primary MC carbides during solidification, as these can negatively influence the mechanical properties.

The chemical composition (Tab. 1) was measured by optical emission spectrometry with inductively coupled plasma ICP-OES Agilent 720 and infrared absorption after combustion with ELTRA CS-800.

**Tab.1** - The chemical composition of the samples is given in percent by weight.

| Sample | C | Si | Ni | Mo | W | Nb | Ta | Ti | Fe |
|---|---|---|---|---|---|---|---|---|---|
| 0 | 0.32 | 0.04 | 0.03 | 3.2 | 1.7 | / | / | / | balance |
| Nb | 0.32 | 0.05 | 0.03 | 3.2 | 1.7 | 0.06 | / | / | balance |
| Ta | 0.32 | 0.05 | 0.03 | 3.2 | 1.7 | / | 0.03 | / | balance |
| Ti | 0.32 | 0.04 | 0.03 | 3.2 | 1.7 | / | / | 0.006 | balance |

The ingots were annealed at 720 °C to relieve stress, then homogenized at 1200 °C for 1 h and hot rolled into 40 x 40 mm billets. After hot rolling, the billets air cooled. The billets were then additionally heated to 1100 °C and hot forged into 18 x 18 mm square bars. The bars were also air cooled. After cooling to room temperature, samples were soft annealed for 1.5 h at 770 °C.

Then the samples were cut to the dimensions 18 x 18 x 60 mm. The hardening process was carried out in an electric resistance laboratory furnace with air atmosphere followed by oil quenching. The samples were placed in a furnace at room temperature, heated to 650 °C in 1 h and held for 20 min, then heated to 850 °C in 30 min and held again for 20 min and then heated to the quenching temperature in 45 min and held for 20 min. The quenching temperatures were 1030, 1060, 1080 and 1100 °C. The oil temperature was 60 °C. After oil quenching, the samples were tempered in a vacuum hardening furnace (Ipsen Turbo XL) under a protective atmosphere at temperatures of 540, 580, 600, 620 and 640 °C with a holding time of 2.5 h. The 2 mm of the surface layer were removed to avoid the influence of decarburisation.

The metallographic samples were ground, polished and etched with Nital 5%. The microstructure was analysed with an Olympus DP70 light microscope and a Thermo Scientific Quattro S field-emission scanning electron microscope with electron dispersive x-ray spectroscopy (EDS). Hardness values were measured on all investigated

samples using Vickers hardness method, HV10.
The commercial software Thermo-Calc version 2022b was used for the CALPHAD calculations. The Thermo-Calc Software TCFE10 Steels/Fe-alloys database was selected to obtain the thermodynamic data for the calculations. We used the Equilibrium Calculator and selected the Property Diagram calculation type, from which we obtained diagrams showing the amount of thermodynamically stable phases in the samples studied.

## RESULTS AND DISCUSSION

The results of CALPHAD calculations are summarized in Tab. 2. Thermodynamically stable phases of the investigated samples were calculated in the temperature range between 500 and 1300 °C. The Thermo-Calc designations are given with the corresponding phase and precipitation or transformation temperatures. It is evident that the addition of microalloying elements (Nb, Ta and Ti) has no effect on the transformation temperature between ferrite and austenite (Ae3 and Ae1). It also has no influence on the precipitation temperature MC (WC), which is basically the same for all the samples studied. A slight influence on the precipitation temperature of the M6C carbides can be seen, with the addition of Nb increasing the temperature by 9 °C. The addition of Ti and Ta, on the other hand, has no influence on the precipitation temperature of the M6C carbides. The main difference is the precipitation of additional carbides based on the microalloying elements. In the Nb sample, there is additional precipitation of MC (NbC) carbides, which start to precipitate at 1253 °C. The same happens with the Ta and Ti samples, where TaC carbides start to precipitate at 1172 °C and TiC at 1057 °C.

**Tab.1** - The chemical composition of the samples is given in percent by weight.

| Sample | Thermo-Calc designation | Phase | Precipitation or transformation temperature (°C) |
|---|---|---|---|
| 0 | FCC_A1#2 | / | / |
| | M6C_E93 | $(Mo, Fe, W)_6C$ | 1087 |
| | MC_SHP | WC | 810 |
| | BCC_A2 | ferrite (α) | 858 – $A_{e3}$ |
| | FCC_A1 | austenite (γ) | 797 – $A_{e1}$ |
| Nb | FCC_A1#2 | NbC | 1253 |
| | M6C_E93 | $(Mo, Fe, W, Nb)_6C$ | 1096 |
| | MC_SHP | WC | 809 |
| | BCC_A2 | ferrite (α) | 860 – $A_{e3}$ |
| | FCC_A1 | austenite (γ) | 797– $A_{e1}$ |
| Ta | FCC_A1#2 | TaC | 1172 |
| | M6C_E93 | $(Mo, Fe, W, Ta)_6C$ | 1087 |
| | MC_SHP | WC | 810 |
| | BCC_A2 | ferrite (α) | 859 – $A_{e3}$ |
| | FCC_A1 | austenite (γ) | 797 – $A_{e1}$ |
| Ti | M6C_E93 | $(Mo, Fe, W, Ti)_6C$ | 1087 |
| | FCC_A1#2 | TiC | 1057 |
| | MC_SHP | WC | 810 |
| | BCC_A2 | ferrite (α) | 859 – $A_{e3}$ |
| | FCC_A1 | austenite (γ) | 797 – $A_{e1}$ |

The quenched and tempered samples exhibit a bainitic-martensitic microstructure. Furthermore, all samples were free of primary carbides.
The hardness of the steel generally increases with higher austenitisation temperatures (as shown in Fig. 1). At an austenitisation temperature of 1030°C, the steel without microalloying elements (0) exhibits an average hardness of 425 HV10. The addition of Nb and Ta did not affect

the increase in hardness at the given austenitisation temperature. However, the addition of titanium (Ti) was effective in increasing the hardness of the steel even at a lower temperature, resulting in an average value of 446 HV10 after quenching.

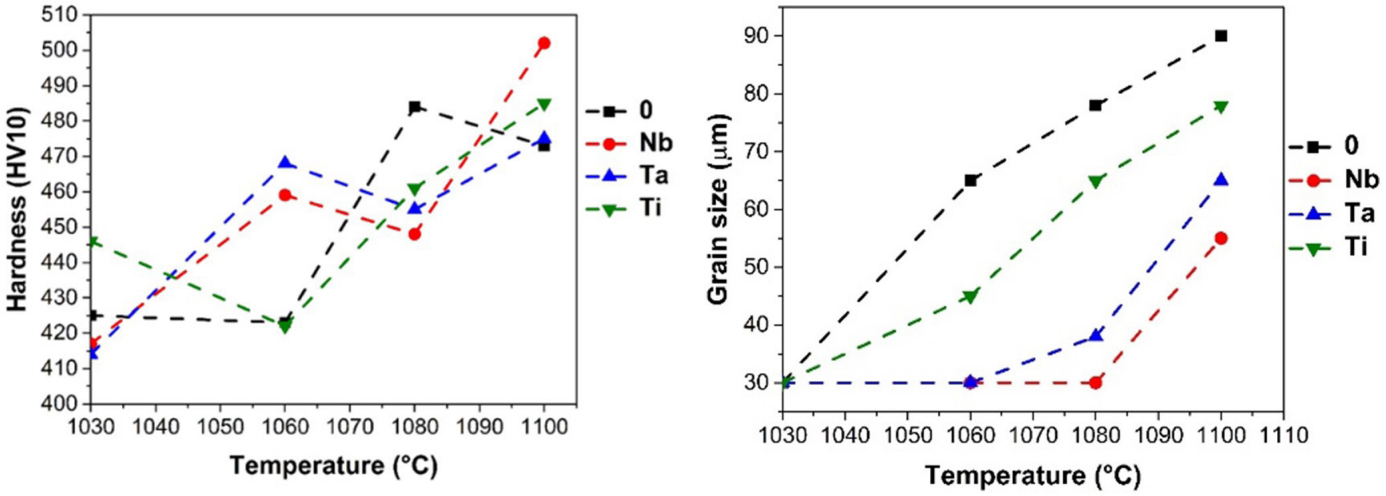


**Fig. 1** - a) Hardness as a function of austenitisation temperature, b) grain size as a function of austenitisation temperature.

The increase in the austenitisation temperature affected the increase in the size of the primary austenite crystal grains, especially of the reference sample (0) and the titanium-alloyed sample (Ti). Samples alloyed with niobium (Nb) and with tantalum (Ta) had a lesser effect on growth. At the highest austenitisation temperature of 1100 °C, all samples developed a coarse-grained microstructure. The hardness is most influenced by the change in the chemistry of the austenite matrix before quenching, the resulting bainite/martensite ration and the grain size. Examples of fine and coarse grained microstructures are presented in Fig. 2. The addition of niobium (Nb) and tantalum (Ta) had a large influence on the size of the crystal grains, which is also consistent with findings from literature sources [28,29]. A more detailed discussion on the grain growth mechanism in the samples is available in our previous work [5].

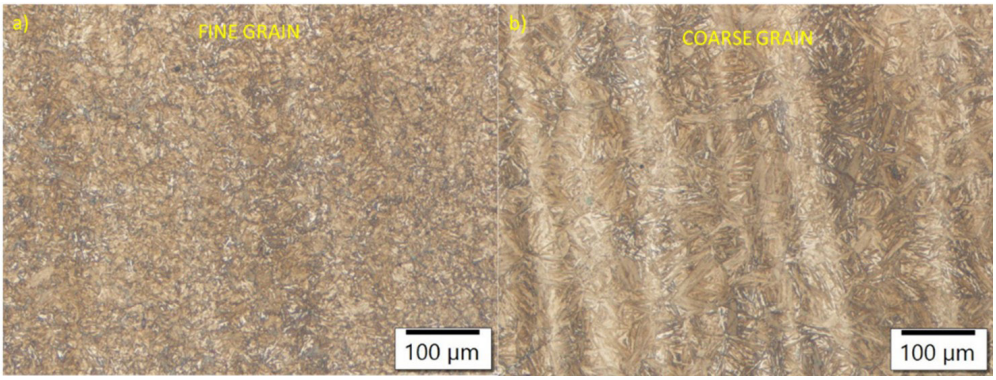


**Fig. 2** - Representative microstructures of a) fine grain sample Ta – 1060 °C and b) coarse grain sample 0 – 1100 °C.

The samples were hardened at austenitising temperatures of 1030, 1060, 1080 and 1100 °C and tempered at temperatures of 540, 580, 600, 620 and 640 °C, which are most commonly used to temper tools to the required hardness. As mentioned before, the tempering times were 2.5 h after reaching temperature. With increasing tempering temperature, a secondary hardness peak was reached in all samples. With increasing austenitisation temperature, the hardness after tempering and the value of the secondary peak hardness also increased. The highest secondary peak hardness values were achieved in the austenitisation temperature interval between 1080 and 1100 °C. The

alloying elements niobium, tantalum and titanium had an influence on the increase of the strength properties in the temperature range between 540 and 640 °C. At an austenitisation temperature of 1030 °C (Fig. 3a), the Ti sample exhibits the maximum secondary peak hardness of 506 HV10. At the austenitisation temperature of 1060 °C (Fig. 3b), the maximum secondary peak hardness of the Nb sample is 533 HV10. At an austenitisation temperature of 1080 °C (Fig. 3c), the maximum secondary peak hardness of Ti sample is 540 HV10. At an austenitisation temperature of 1100 °C (Fig. 3d), the maximum secondary peak hardness of Nb and Ti samples is 542 HV.

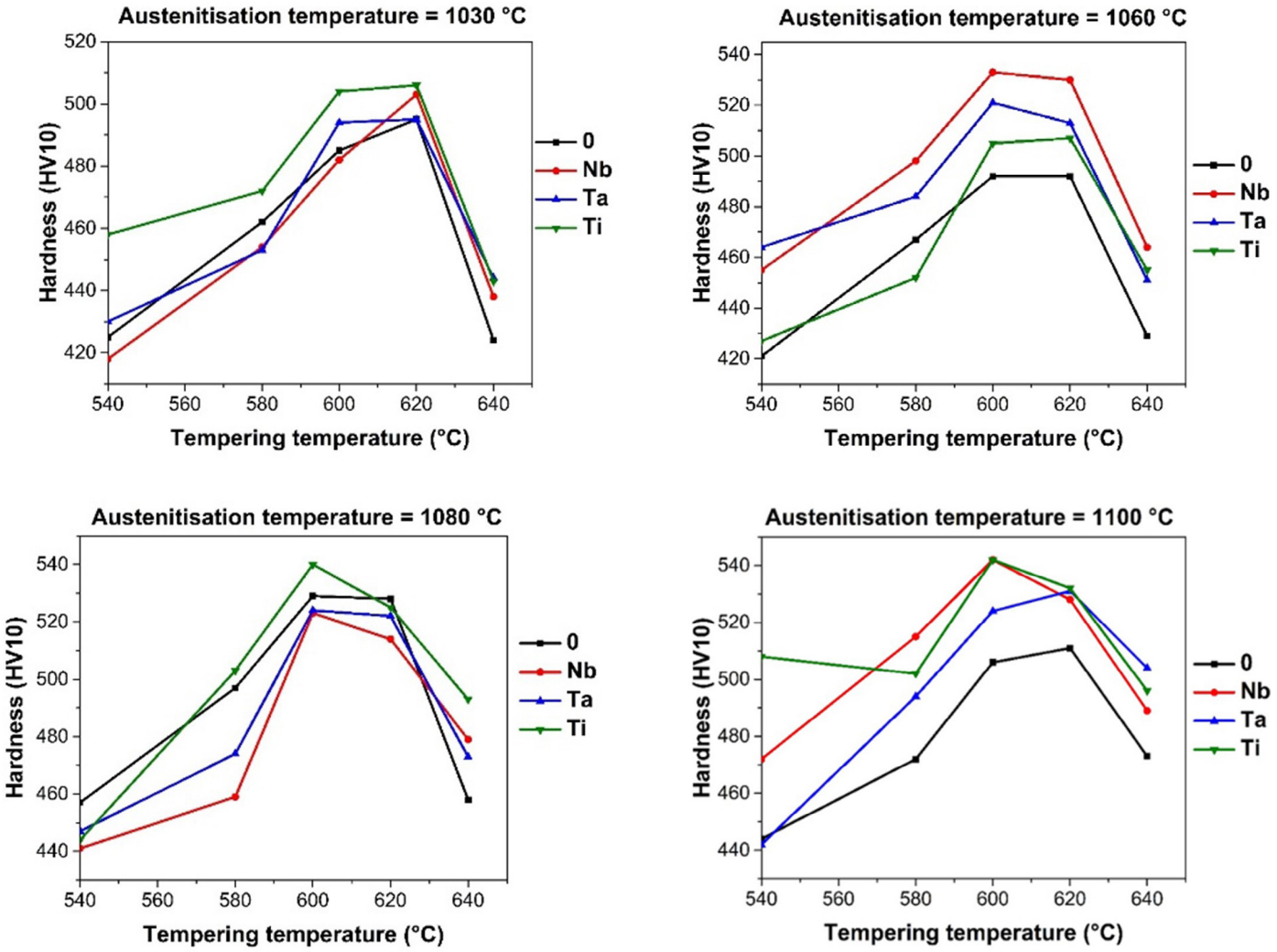


**Fig. 3** - Tempering diagram for all the samples at different austenitisation temperatures a) 1030 °C, b) 1060 °C, c) 1080 °C, d) 1100 °C.

## CONCLUSIONS

The following conclusions can be drawn from the paper:

- The microalloying elements, especially Nb and Ta were effective at pinning grain boundaries during austenitisation, up to 1100 °C.
- The secondary hardening peak for Mo-W high thermal conductivity steel is between 600 and 620 °C, for all the investigated heat treatment regimes.
- The microalloying elements influenced the hardness after tempering, mostly by increasing it, especially at the lowest 1030 °C and the highest 1080 °C austenitisation temperatures.

## REFERENCES

[1] Eser, A.; Broeckmann, C.; Simsir, C. Multiscale modeling of tempering of AISI H13 hot-work tool steel - Part 1: Prediction of microstructure evolution and coupling with mechanical properties. Comput. Mater. Sci. 2016, 113, 280–291.
[2] Li, J. Y.; Chen, Y. L.; Huo, J. H. Mechanism of improvement on strength and toughness of H13 die steel by nitrogen. Mater. Sci. Eng. A 2015, 640, 16–23.
[3] Wu, R.; Li, W.; Chen, M.; Huang, S.; Hu, T. Improved mechanical properties by nanosize tungsten-molybdenum carbides in tungsten containing hot work die steels. Mater. Sci. Eng. A 2021, 812, 141140.
[4] Markežič, R.; Mole, N.; Naglič, I.; Šturm, R. Time and temperature dependent softening of H11 hot-work tool steel and definition of an anisothermal tempering kinetic model. Mater. Today Commun. 2020, 22.
[5] Grabnar, Klemen; Burja, Jaka; Balaško, Tilen; Nagode, Aleš; Medved, J. The influence of Nb, Ta and Ti modification on hot-work tool-steel grain growth during austenitization. Mater. Technol. 2022, 56, 331–338.
[6] Vončina, M.; Balaško, T.; Medved, J.; Nagode, A. Interface reaction between molten Al99.7 aluminum alloy and various tool steels. Materials. 2021, 14.
[7] De Cooman, B. C.; Speer, J. G. Fundamentals of Steel Product Physical Metallurgy; AIST, Association for Iron & Steel Technology: Warrendale, PA, USA, 2011.
[8] Podgornik, B.; Sedlacek, M.; Žužek, B.; Guštin, A. Properties of tool steels and their importance when used in a coated system. Coatings 2020, 10.
[9] Zhou, Q.; Wu, X.; Shi, N.; Li, J.; Min, N. Microstructure evolution and kinetic analysis of DM hot-work die steels during tempering. Mater. Sci. Eng. A 2011, 528, 5696–5700.
[10] Medvedeva, A.; Bergström, J.; Gunnarsson, S.; Andersson, J. High-temperature properties and microstructural stability of hot-work tool steels. Mater. Sci. Eng. A 2009, 523, 39–46.
[11] Dhokey, N. B.; Maske, S. S.; Ghosh, P. Effect of tempering and cryogenic treatment on wear and mechanical properties of hot work tool steel (H13). Mater. Today Proc. 2021, 43, 3006–3013.
[12] Cabrol, E.; Bellot, C.; Lamesle, P.; Delagnes, D.; Povoden-Karadeniz, E. Experimental investigation and thermodynamic modeling of molybdenum and vanadium-containing carbide hardened iron-based alloys. J. Alloys Compd. 2013, 556, 203–209.
[13] Chen, K.; Jiang, Z.; Liu, F.; Yu, J.; Li, Y.; Gong, W.; Chen, C. Effect of quenching and tempering temperature on microstructure and tensile properties of microalloyed ultra-high strength suspension spring steel. Mater. Sci. Eng. A 2019, 766.
[14] Yang, G.; Sun, X.; Li, Z.; Li, X.; Yong, Q. Effects of vanadium on the microstructure and mechanical properties of a high strength low alloy martensite steel. Mater. Des. 2013, 50, 102–107.
[15] Zhang, C.; Wang, Q.; Ren, J.; Li, R.; Wang, M.; Zhang, F.; Sun, K. Effect of martensitic morphology on mechanical properties of an as-quenched and tempered 25CrMo48V steel. Mater. Sci. Eng. A 2012, 534, 339–346.
[16] Wang, C.; Wang, M.; Shi, J.; Hui, W.; Dong, H. Effect of microstructural refinement on the toughness of low carbon martensitic steel. Scr. Mater. 2008, 58, 492–495.
[17] Haiko, O.; Javaheri, V.; Valtonen, K.; Kaijalainen, A.; Hannula, J.; Kömi, J. Effect of prior austenite grain size on the abrasive wear resistance of ultra-high strength martensitic steels. Wear 2020, 454–455, 13–16.
[18] Karmakar, A.; Kundu, S.; Roy, S.; Neogy, S.; Srivastava, D.; Chakrabarti, D. Effect of microalloying elements on austenite grain growth in Nb-Ti and Nb-V steels. Mater. Sci. Technol. (United Kingdom) 2014, 30, 653–664.
[19] Hollomon, J.H; Jaffe, L. D. TitleTime–temperature relations in tempering steels; 1975; Vol. 162.
[20] Mazurkiewicz, J.; Dobrzański, L. A.; Hajduczek, E. Comparison of the secondary hardness effect after tempering of the hot-work tool steels. 2007, 24, 119–122.
[21] Leskovšek, V.; Šuštaršič, B.; Jutriša, G. The influence of austenitizing and tempering temperature on the hardness and fracture toughness of hot-worked H11 tool steel. J. Mater. Process. Technol. 2006, 178, 328–334.
[22] Yang, H.; Zhang, J. H.; Xu, Y.; Meyers, M. A. Microstructural characterization of the shear bands in Fe-Cr-Ni single crystal by EBSD. J. Mater. Sci. Technol. 2008, 24, 819–828.
[23] Janovec, J.; Svoboda, M.; Výrostková, A.; Kroupa, A. Time-temperature-precipitation diagrams of carbide evolution in low alloy steels. Mater. Sci. Eng. A 2005, 402, 288–293.
[24] Jung, J. G.; Park, J. S.; Kim, J.; Lee, Y. K. Carbide precipitation kinetics in austenite of a Nb-Ti-V microalloyed steel. Mater. Sci. Eng. A 2011, 528, 5529–5535.
[25] Dong, J.; Zhou, X.; Liu, Y.; Li, C.; Liu, C.; Guo, Q. Carbide precipitation in Nb-V-Ti microalloyed ultra-high strength steel during tempering. Mater. Sci. Eng. A 2017, 683, 215–226.
[26] Kaschnitz, E.; Hofer, P.; Funk, W. Thermophysical properties of a hot-work tool-steel with high thermal conductivity. Int. J. Thermophys. 2013, 34, 843–850.
[27] Valls, I.; Hamasaiid, A.; Padré, A. High Thermal Conductivity and High Wear Resistance Tool Steels for cost-effective Hot Stamping Tools. J. Phys. Conf. Ser. 2017, 896.
[28] Chen, J.; Liu, C.; Liu, Y.; Yan, B.; Li, H. Effects of tantalum content on the microstructure and mechanical properties of low-carbon RAFM steel. J. Nucl. Mater. 2016, 479, 295–301.
[29] Foder, J.; Burja, J.; Klančnik, G. Grain size evolution and mechanical properties of Nb, V–Nb, and Ti–Nb boron type S1100QL steels. Metals. 2021, 11, 1–16.

TORNA ALL'INDICE >